

An EAR-Dependent Regulatory Module Promotes Male Germ Cell Division and Sperm Fertility in *Arabidopsis*

Michael Borg,^a Nicholas Rutley,^a Sateesh Kagale,^b Yuki Hamamura,^c Mihai Gherghinoiu,^a Sanjeev Kumar,^a Ugur Sari,^a Manuel A. Esparza-Franco,^a Wataru Sakamoto,^d Kevin Rozwadowski,^b Tetsuya Higashiyama,^{c,e} and David Twell^{a,1}

^aDepartment of Biology, University of Leicester, Leicester LE1 7RH, United Kingdom

^bAgriculture and Agri-Food Canada, Saskatoon SK S7N 0X2, Canada

^cJST, ERATO, Higashiyama Live-Holonics Project, Nagoya University, Furo-cho, Chikusa-ku, Nagoya, Aichi 464-8602, Japan

^dInstitute of Plant Science and Resources, Okayama University, Kurashiki, Okayama 710-0046, Japan

^eInstitute of Transformative Bio-Molecules, Nagoya University, Furo-cho, Chikusa-ku, Nagoya, Aichi 464-8602, Japan

ORCID IDs: 0000-0002-3982-3843 (M.B.); 0000-0003-0483-1461 (D.T.)

The production of the sperm cells in angiosperms requires coordination of cell division and cell differentiation. In *Arabidopsis thaliana*, the germline-specific MYB protein DUO1 integrates these processes, but the regulatory hierarchy in which DUO1 functions is unknown. Here, we identify an essential role for two germline-specific DUO1 target genes, *DAZ1* and *DAZ2*, which encode EAR motif-containing C₂H₂-type zinc finger proteins. We show that *DAZ1/DAZ2* are required for germ cell division and for the proper accumulation of mitotic cyclins. Importantly, *DAZ1/DAZ2* are sufficient to promote G2- to M-phase transition and germ cell division in the absence of DUO1. *DAZ1/DAZ2* are also required for DUO1-dependent cell differentiation and are essential for gamete fusion at fertilization. We demonstrate that the two EAR motifs in *DAZ1/DAZ2* mediate their function in the male germline and are required for transcriptional repression and for physical interaction with the corepressor TOPLESS. Our findings uncover an essential module in a regulatory hierarchy that drives mitotic transition in male germ cells and implicates gene repression pathways in sperm cell formation and fertility.

INTRODUCTION

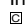
The germline is the lineage of cells that produces the gametes and transmits genetic material from one generation to the next. In animals, a discrete germline is segregated from somatic cells early during embryogenesis, whereas an equivalent germline is challenging to define in plants, as somatic stem cells give rise to male and female germ cell lineages that only differentiate late in development (Dickinson and Grant-Downton, 2009; Berger and Twell, 2011). In flowering plants, this occurs after formation of the floral organs, in which separate meiosis give rise to haploid unicellular male and female gametophytes, the microspores and megaspores, which undergo distinct germline developmental programs to form the gametes. The male germline is segregated in the gametophyte by asymmetric division of the microspore to form the generative (germ) cell, which rapidly establishes a distinct developmental program. This male germ cell then completes a mitotic division and differentiates to form the two sperm cells required for double fertilization (Borg et al., 2009). In contrast, the female germline is only segregated after three rounds of nuclear division followed by cellularization of the embryo sac (Yadegari and Drews, 2004).

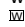
There have been major advances in our understanding of the events regulating germline development and gamete specification in angiosperms (Berger and Twell, 2011; Twell, 2011). The cellularization and differentiation of cells in the embryo sac appear to be transcriptionally regulated (Rabiger and Drews, 2013), and mechanisms involving RNA splicing and auxin and peptide signaling specify female gametic cells (Gross-Hardt et al., 2007; Pagnussat et al., 2009; Lieber et al., 2011; Lituiev et al., 2013). For male germline development, a regulatory framework for cell cycle progression and gamete specification has been established (Brownfield and Twell, 2009; Borg and Twell, 2010; Twell, 2011). Timely progression of the generative cell cycle requires the control of cyclin-dependent kinase activity by the F-box protein FBL17, which targets cyclin-dependent kinase inhibitory proteins for degradation (Kim et al., 2008; Gusti et al., 2009). In parallel, the male germline-specific MYB transcription factor DUO POLLEN1 (DUO1) integrates division of the generative cell with differentiation of the sperm cells (Rotman et al., 2005; Brownfield et al., 2009a; Borg et al., 2011).


DUO1 promotes germ cell division by regulating the G2 accumulation of the mitotic cyclin CYCB1;1 and is required for the expression of genes that are essential for differentiation of sperm cells (Brownfield et al., 2009a). The target genes that constitute the DUO1 regulon were identified by ectopic expression of DUO1 in seedlings (Borg et al., 2011). In contrast, *CYCB1;1* transcripts are not induced by DUO1 in seedlings, and the expression of *CYCB1;1* in mutant *duo1* germ cells only partially rescues failed division (Brownfield et al., 2009a), indicating that the role of DUO1 in G2- to M-phase transition is complex. This raises important questions about the underlying regulatory mechanisms and how

¹ Address correspondence to twe@le.ac.uk.

The author responsible for distribution of materials integral to the findings presented in this article in accordance with the policy described in the Instructions for Authors (www.plantcell.org) is: David Twell (twe@le.ac.uk).

 Some figures in this article are displayed in color online but in black and white in the print edition.

 Online version contains Web-only data.

 Articles can be viewed online without a subscription.

www.plantcell.org/cgi/doi/10.1105/tpc.114.124743

they are integrated with gamete specification. First, are transcript or protein levels the primary cause of failed CYCB1;1 accumulation? Second, what are the regulatory nodes that promote germ cell mitosis in the DUO1 network and do they act independently of cell differentiation?

Here, we answer these questions and provide insights into the regulatory hierarchy of male gametogenesis in flowering plants. We focused our attention on two genes encoding C₂H₂-type zinc finger proteins (ZFPs), *DUO1-ACTIVATED ZINC FINGER1 (DAZ1)* and *DAZ2*, that were induced by DUO1 in seedlings and show DUO1-dependent expression in sperm cells (Borg et al., 2011). *DAZ1* and *DAZ2* form a distinct clade among C₂H₂-type ZFPs with each containing leucine-rich ETHYLENE RESPONSE FACTOR-associated amphiphilic repression (EAR) motifs (Englbrecht et al., 2004). The plant Groucho/Tup1 corepressor family of TOPLESS/TOPLESS RELATED (TPL/TPR) proteins mediate the repressor activity of different EAR-containing proteins by acting upon chromatin via histone deacetylases (Szemenyei et al., 2008; Pauwels et al., 2010; Kagale and Rozwadowski, 2011). Furthermore, although the *Arabidopsis thaliana* TPL/TPR interactome has been reported (Causier et al., 2012), there is little evidence for the role of transcriptional repression pathways in germline development.

We show that DUO1 regulates *DAZ1* and *DAZ2* transcription through conserved promoter motifs and that *DUO1* and *DAZ1/DAZ2* are developmentally regulated in the germline of *Arabidopsis*. *DAZ1/DAZ2* are required for germ cells to enter mitosis and for the proper accumulation of mitotic cyclins. We show that *DAZ1* and *DAZ2* are required for the correct expression of male germline differentiation genes and for the competence of sperm in fertilization. We show that *DAZ1* and *DAZ2* physically interact with the corepressor TPL, and the EAR domain of *DAZ1* can mediate transcriptional repression in planta. Significantly, the EAR motifs have an important role in the functions of *DAZ1*, and our results support a model in which the DUO1-*DAZ1/DAZ2* module promotes mitotic entry and ensures correct germ cell differentiation through EAR-mediated mechanisms.

RESULTS

DAZ1 and DAZ2 Are Male Germline-Specific Nuclear Proteins Directly Regulated by DUO1

DAZ1 and *DAZ2* form a distinct subgroup (C1-3iC) within the C₂H₂-type ZFP family that are characterized by three dispersed zinc finger domains and a conserved CLLM amino acid motif between the first and second zinc fingers (Figure 1A) (Englbrecht et al., 2004). Phylogenetic analysis identified putative orthologs in eudicots with three conserved zinc finger domains (Supplemental Figure 1). Homologous sequences are present in monocots, although these lack the second zinc finger domain and putative NLS (Supplemental Figure 1). In addition to the zinc finger domains, we identified extended conservation around the CLLM motif and the tandem DLNxxP- and LxLxL-type EAR motifs at the C terminus (Figure 1A) (Kagale et al., 2010).

We investigated the expression of *DAZ1* and *DAZ2* in developing pollen by generating transgenic protein fusion lines, ProDAZ1:

DAZ1-mCherry and ProDAZ2:*DAZ2*-mCherry. Fluorescence signals were absent in microspores and first appeared in the germ cell nucleus following microspore division (Figure 1B). The germline-specific signal increased during development and persisted into mature pollen (Figure 1B), which mirrored the activity of the corresponding promoter marker lines, ProDAZ1:*H2B*-GFP (green fluorescent protein) and ProDAZ2:*H2B*-GFP (Supplemental Figure 2). In mature pollen, *DAZ2*-mCherry fluorescence was present exclusively in sperm cell nuclei (Supplemental Figure 3). *DAZ1*-mCherry fluorescence was nuclear-enriched, but also present in the cytoplasm of the majority of sperm cells (Supplemental Figure 3). When we analyzed sporophytic tissues by RT-PCR, *DAZ1* and *DAZ2* transcripts were only detected in pollen (Supplemental Figure 4).

DUO1 activates its direct target genes by binding to MYB binding sites (MBSs) in their promoter regions (Borg et al., 2011). We mutagenized the MBSs present in the *DAZ1* and *DAZ2* promoter regions and examined the effect on DUO1-dependent transactivation in transient expression assays. Relative to native *DAZ1* and *DAZ2* promoter fragments, independent mutagenesis of each MBS resulted in substantially decreased luciferase activities. These data confirm the importance of MBSs in the *DAZ1* and *DAZ2* promoters and support a direct role for DUO1 in *DAZ1* and *DAZ2* transcription (Figures 2A and 2B).

We explored the developmental expression profiles for *DUO1*, *DAZ1*, and *DAZ2* by assaying transcript and protein abundance. Transcripts were measured by quantitative RT-PCR (qRT-PCR) analysis of RNA isolated from spores at four stages of pollen development. *DUO1* transcripts reached maximum levels in bicellular pollen before declining in tricellular and mature pollen (Figure 1C). *DAZ1* and *DAZ2* transcripts, however, reached a peak in tricellular pollen before declining in mature pollen (Figure 1C). The highest levels of DUO1-mCherry fluorescence were measured in germ cells immediately before division, decreasing in sperm cells (Figure 1D). In contrast, the fluorescence of *DAZ1*-mCherry and *DAZ2*-mCherry peaked in newly formed sperm cells, declining thereafter (Figure 1D). These developmentally phased expression profiles provide compelling evidence that DUO1 directly determines the male germline-specific accumulation of *DAZ1* and *DAZ2*.

DAZ1 and DAZ2 Mediate the Regulation of Germ Cell Division by DUO1

To investigate the functional role of *DAZ1* and *DAZ2*, we searched for T-DNA insertion lines and identified two insertions in the coding region of *DAZ1* and a single insertion in the proximal promoter region of *DAZ2* (Figure 1A). RT-PCR analysis failed to detect the corresponding transcripts in *daz1-2*^{-/-} and *daz2-1*^{-/-} pollen, whereas residual transcript was detected in *daz1-1*^{-/-} pollen (Supplemental Figure 5). Homozygous knockout lines for *DAZ1* or *DAZ2* did not show abnormal vegetative or reproductive phenotypes, while self-progeny of heterozygous mutants segregated ~3:1 for T-DNA-derived kanamycin resistant-to-sensitive seedlings (*n* > 380). When heterozygous *daz1* and *daz2* mutants were crossed to *male sterile1-1 (ms1-1)* pistils, the progeny did not deviate significantly from a 1:1 ratio, indicating that single insertion mutants do not cause male transmission defects (*n* > 300).

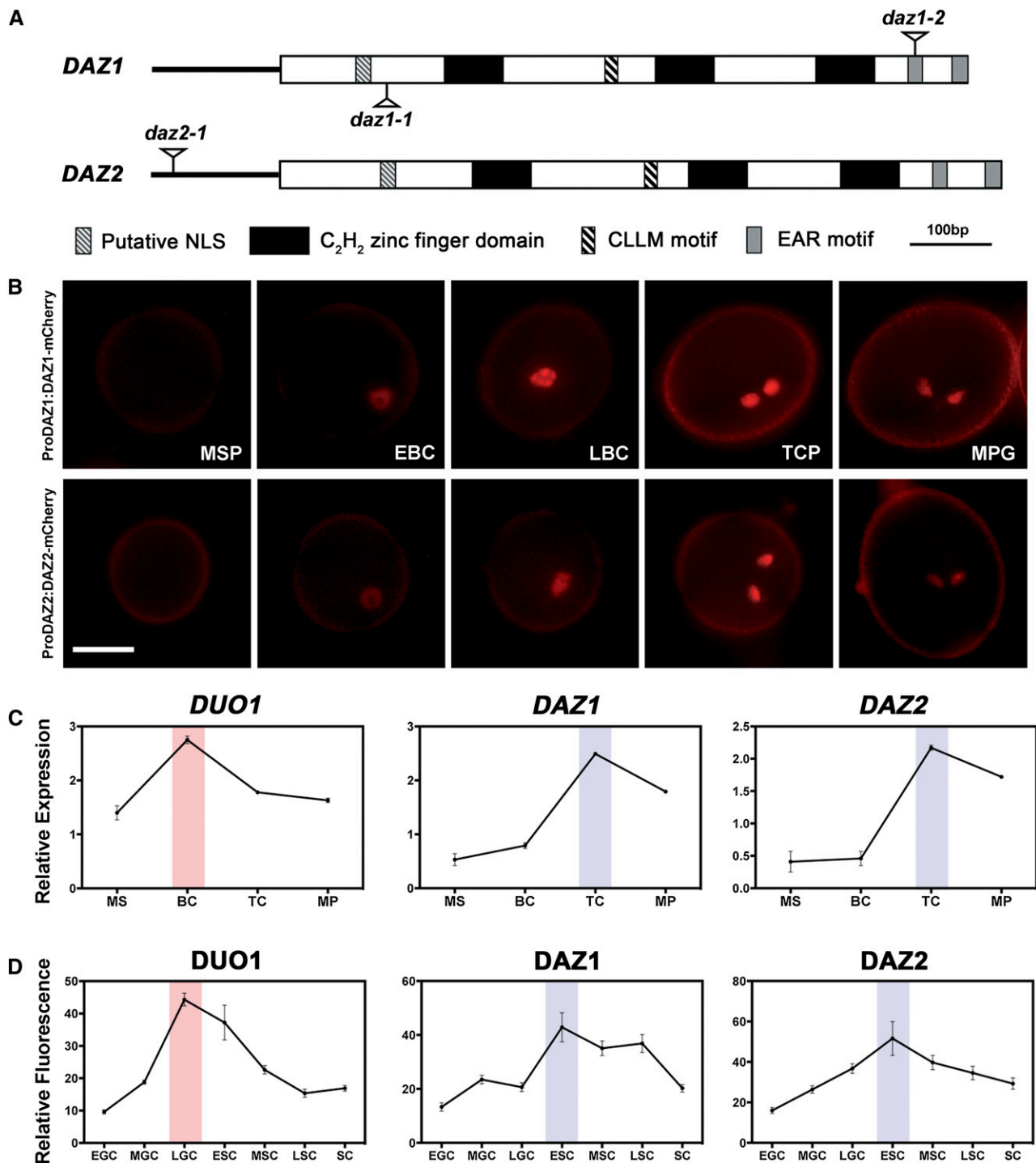


Figure 1. DAZ1 and DAZ2 Encode Male Germline-Specific EAR Motif-Containing C_2H_2 -Type Zinc Finger Proteins.

(A) Schematic diagram of the *DAZ1* and *DAZ2* loci. The locations of three dispersed C_2H_2 -type zinc finger domains, a putative nuclear localization signal, a conserved CLLM(L/M) motif, and two EAR motifs are marked. T-DNA insertion sites for the *daz1-1*, *daz1-2*, and *daz2-1* mutant alleles are indicated.

(B) Expression of ProDAZ1:DAZ1-mCherry and ProDAZ2:DAZ2-mCherry during pollen development. MSP, microspore; EBC, early bicellular; LBC, late bicellular; TCP, tricellular pollen; MPG, mature pollen grains. Bar = 15 μ m.

(C) Relative transcript levels of *DUO1*, *DAZ1*, and *DAZ2* determined by qRT-PCR analysis of microspore (MS), bicellular pollen (BC), tricellular pollen (TC), and mature pollen (MP) samples. Shading indicates the earlier peak of *DUO1* transcripts (pink) compared with *DAZ1* and *DAZ2* (blue). Error bars represent the \pm SE of three technical replicates.

(D) Developmental expression of *DUO1*, *DAZ1*, and *DAZ2* fusion proteins in the germline. Fluorescence of developing germ cells from ProDUO1:DUO1-mRFP, ProDAZ1:DAZ1-mCherry, and ProDAZ2:DAZ2-mCherry lines is shown (see Methods). Error bars represent the \pm SE. Shading indicates the earlier peak of *DUO1* protein (pink) compared with *DAZ1* and *DAZ2* (blue). EGC, MGC, LGC, early, mid, late germ cell; ESC, MSC, LSC, early, mid, late spermatocyte; SC, mature sperm cell.

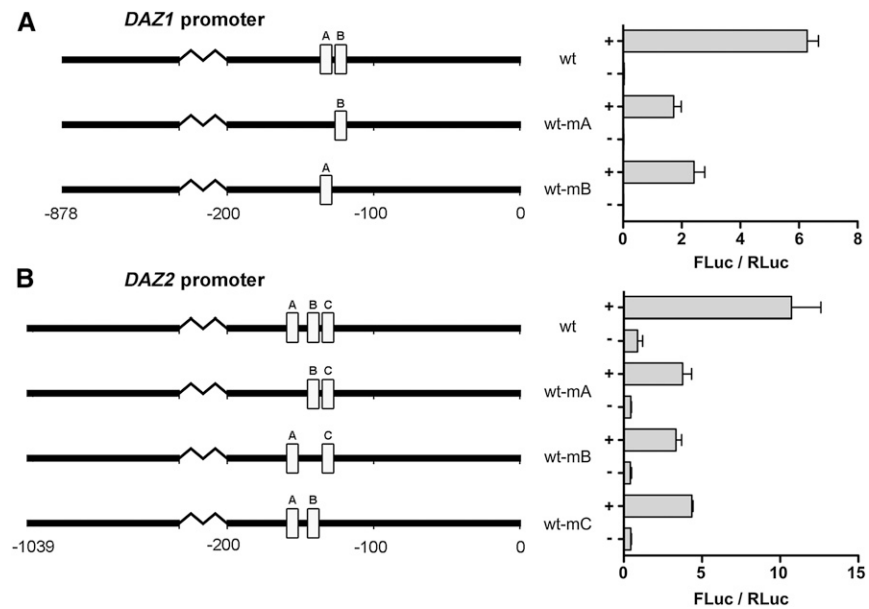


Figure 2. MYB Binding Sites Are Essential for DUO1-Dependent Transactivation of the *DAZ1* and *DAZ2* Promoters.

Schematic diagrams (left) of wild-type and mutated *DAZ1* (A) and *DAZ2* (B) promoter fragments used in trans-activation assays by agroinfiltration of tobacco (*Nicotiana tabacum*) leaves. The positions of the intact MYB sites remaining are indicated (white boxes). The mean relative activities (FLuc/RLuc) shown are from at least four independent experiments; error bars indicate the SE. The “+/-” indicates the presence or absence of 35S:DUO1 expressing strains.

Intriguingly, when each of the *daz1-1* or *daz1-2* alleles were combined with the *daz2-1* allele, we observed a class of pollen grains with a single germ cell-like nucleus similar to mutant *duo1* pollen (Figures 3B and 3D). The *daz1 daz2* mutant phenotype was fully penetrant for both allele combinations: Double heterozygous mutants showed ~25% bicellular pollen and homozygous-heterozygous mutants ~50% bicellular pollen ($n > 500$). Moreover, the *daz1 daz2* mutant phenotype was complemented in lines expressing a ProDAZ1:DAZ1-mCherry transgene (Table 1; see below). These results demonstrate that *DAZ1* and *DAZ2* act redundantly and are required for division of the generative cell.

We focused further characterization on comparison of the *daz1 daz2* mutants with *duo1-4*, since mutant alleles in both genes are in the Columbia-0 (Col-0) background. We examined ultrathin sections of pollen grains by transmission electron microscopy and confirmed that *daz1 daz2* mutant germ cells were surrounded by complete plasma membranes (Figures 3E to 3J). The vegetative cell cytoplasm of *daz1 daz2* pollen was indistinguishable from that of the wild type, indicating that the *daz1 daz2* pollen phenotype is restricted to the germline (Figures 3G to 3J). To investigate the stage at which mutant germ cells are defective, nuclear DNA content was estimated by measurement of 4',6-diamidino-2-phenylindole (DAPI) fluorescence relative to germ cell nuclei of the *duo2* mutant that arrests in mitosis (Durbary et al., 2005). The mean relative DNA content of *duo1-4* and *daz1 daz2* germ cells was 2.44 ± 0.06 and $2.74C \pm 0.07$ (\pm SE) respectively, which was significantly greater than that of *duo2* (Figure 3K). Thus, similar to DUO1-deficient germ cells, *DAZ1/DAZ2*-deficient germ cells appear to skip mitosis and reenter S-phase before anthesis.

To determine whether *DAZ1* was sufficient to promote germ cell division in the absence of DUO1, we introduced a ProDUO1:DAZ1-mCherry transgene into *duo1-1*^{+/-} plants (Figures 4A to 4C). In the event of complete rescue of the *duo1-1* germ cell division defect, the percentage of tricellular pollen is predicted to increase from 50 to ~75% for single locus insertions. In four out of six lines examined, we observed full rescue (Figure 4D; Supplemental Table 1). However, we observed a class of pollen containing sperm cells with *DAZ1*-mCherry expression but no ProHTR10:H2B-GFP signal (Figures 4C and 4D). Since *HTR10* is a direct target of DUO1 and a marker of sperm cell fate (Borg et al., 2011), *duo1-1* sperm cells that are rescued by *DAZ1* remain incompletely differentiated. When we used two lines as pollen donors in testcrosses to *ms1-1* pistils, we observed an ~1:1 ratio of T-DNA-derived antibiotic resistant-to-sensitive seedlings in the progeny ($n > 150$). A 1:1 ratio is expected if rescued *duo1-1* pollen fails to transmit the ProDUO1:DAZ1-mCherry transgene. These data show that *DAZ1/DAZ2* are sufficient to promote germ cell division, but not gamete differentiation, in the absence of DUO1.

DAZ1/DAZ2-Dependent Pathways Affect the Accumulation of Mitotic Cyclins

The transition of cells from G2 to mitosis is characterized by the accumulation of a specific class of mitotic or B-type cyclins, and we previously showed that a CYCB1;1-GUS reporter does not accumulate in *duo1* germ cells (Brownfield et al., 2009a). We monitored CYCB1;1 expression in *daz1 daz2* germ cells using

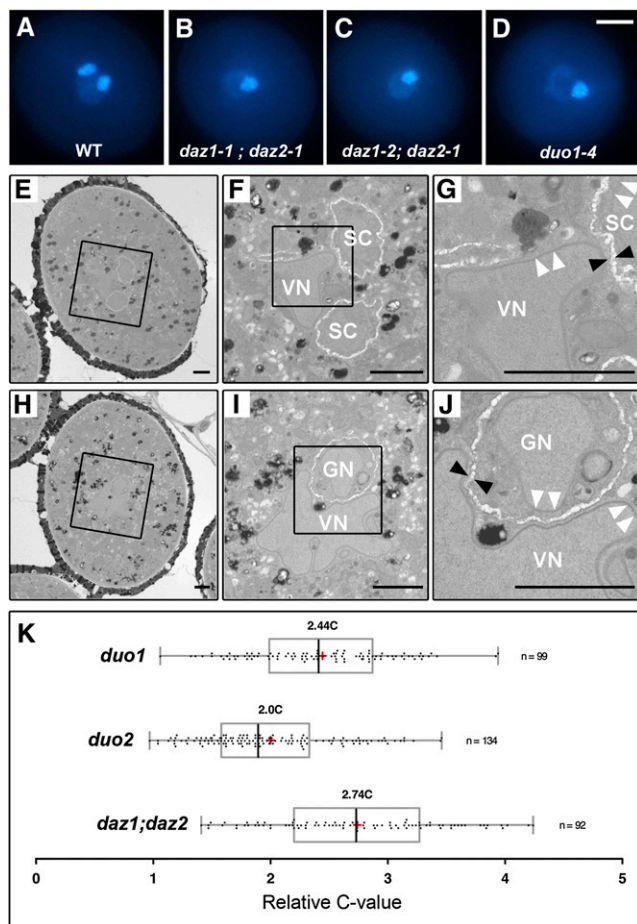


Figure 3. DAZ1 and DAZ2 Are Essential for Division of the Generative Cell.

(A) to (D) Phenotypes of tricellular wild-type (A) and bicellular mutant (B) to (D) pollen genotypes stained with DAPI. Bar = 10 μ m.

(E) to (J) Transmission electron micrographs of wild-type (E) to (G) and *daz1-1 daz2-1* mutant pollen (H) to (J). The boxed regions, magnified left to right, show association of the vegetative cell nucleus and sperm cell (G) or mutant germ cell (J). White arrowheads indicate the nuclear envelope and black arrowheads indicate double membranes enclosing the germline cells. VN, vegetative cell nucleus; GN, mutant germ cell nucleus; SC, sperm cells. Bars = 5 μ m.

(K) Scatter box plot of the relative DNA content of *duo1-4*, *duo2*, and *daz1-1 daz2-1* mutant germ cell nuclei normalized to the DNA content (2.0C) of *duo2* germ cells (Durberry et al., 2005). Both *duo1-4* and *daz1-1 daz2-1* germ cell nuclei had a significantly greater DNA content compared with *duo2* (Tukey-Kramer honestly significantly different, $P < 0.01$) [See online article for color version of this figure.]

a similar CYCB1;1 reporter, ProCYCB1;1:MDB-GFP, in which the CYCB1;1 promoter and N-terminal mitotic destruction box (MDB) are fused to GFP (Brownfield et al., 2009b). To mark germ cell nuclei and to distinguish premitotic and mitotic cells, we used a ProDUO1:H2B-tdTomato transgene since the DUO1 promoter is active in *duo1* (Brownfield et al., 2009a) and in *daz1 daz2* mutant germ cells (see below; Figure 7E). This marker distinguishes condensing chromatin during prophase and fully

condensed and aligned chromosomes at metaphase (Figures 4E to 4G). Consistent with the failure of mutant germ cells to divide, we observed about half the frequency of prophase nuclei in *duo1-1^{+/-}* and *daz1-1^{-/-} daz2^{+/-}* plants compared with wild-type and *daz1-1^{-/-}* plants, in which all germ cells are able to divide (Figure 4H). Pollen from anthers enriched with germ cells undergoing mitosis were scored in lines that were homozygous for both ProCYCB1;1:MDB-GFP and ProDUO1:H2B-tdTomato in a *duo1-1^{+/-}* and *daz1-1^{-/-} daz2-1^{+/-}* background. In wild-type and *daz1-1^{-/-}* plants, GFP was detectable in the nuclei of premitotic germ cells and appeared more intense in cells undergoing mitosis (Figures 5A to 5C). As expected, GFP was undetectable in half of the premitotic cells from *duo1-1^{+/-}* anthers (Figure 5D). In contrast, there was no difference in the proportion of GFP-positive premitotic cells in *daz1-1^{-/-}* and *daz1-1^{-/-} daz2-1^{+/-}* plants (Figure 5D), but the levels of ProCYCB1;1:MDB-GFP fluorescence in double mutants was nearly 2-fold lower (Figure 5E). These data highlight differences in the accumulation of CYCB1;1 in *duo1* and *daz1 daz2* mutant germ cells.

To test the hypothesis that enhanced activity of the anaphase-promoting complex (APC/C) might be the cause of reduced CYCB1;1 accumulation in *duo1* and *daz1 daz2* germ cells, we expressed the CYCB1;1 mitotic destruction box fused to mCherry under control of the DUO1 promoter (ProDUO1:MDB-mCherry) in *duo1* and *daz1 daz2* germ cells. In pollen from several *duo1-4^{+/-}* and *daz1-1^{-/-} daz2-1^{+/-}* T1 plants, we observed persistent MDB-mCherry fluorescence in undivided germ cells that was not evident in sperm cells (Figures 5F and 5G). The frequency of undivided mCherry-positive germ cells in several T1 plants was not significantly different from 25% and consistent with that expected for single locus lines (Figure 5H). At earlier stages of development, we observed twice the number of undivided germ cells that were mCherry positive, and this signal was gradually lost in half of the pollen during maturation (Figure 5I). The accumulation of MDB-mCherry during G2-phase in *duo1* and *daz1 daz2* germ cells strongly suggests that APC/C-dependent turnover is not responsible for the reduced accumulation of CYCB1;1. Furthermore, when we quantified CYCB1;1 and CYCB1;2 transcript levels in pollen of *duo1-4^{+/-}* and *daz1-1^{-/-} daz2-1^{+/-}* mutants, both were significantly reduced relative to the wild type (Figure 5J), consistent with the reduced ProCYCB1;1:MDB-GFP marker expression observed in planta (Figures 5D and 5E).

The germline-targeted expression of CYCB1;1 with the DUO1 promoter was able to partially restore germ cell division in *duo1* (Brownfield et al., 2009a). However, when we introduced the same transgene into double mutant *daz1 daz2* plants, the frequency of bicellular pollen was not significantly affected (Supplemental Table 2). This suggests that *daz1 daz2* germ cells do not fail to divide only as a result of reduced CYCB1;1 transcript accumulation and that other G2/M-promoting and/or inhibitory factors are also involved.

DAZ1/DAZ2-Dependent Pathways Are Also Required for Gamete Differentiation

To investigate the fertility of *daz1 daz2* double mutant pollen, we genotyped the progeny from *daz1-1^{+/-} daz2-1^{+/-}* plants. No

Table 1. The EAR Motifs of DAZ1 Are Important for Germ Cell Division

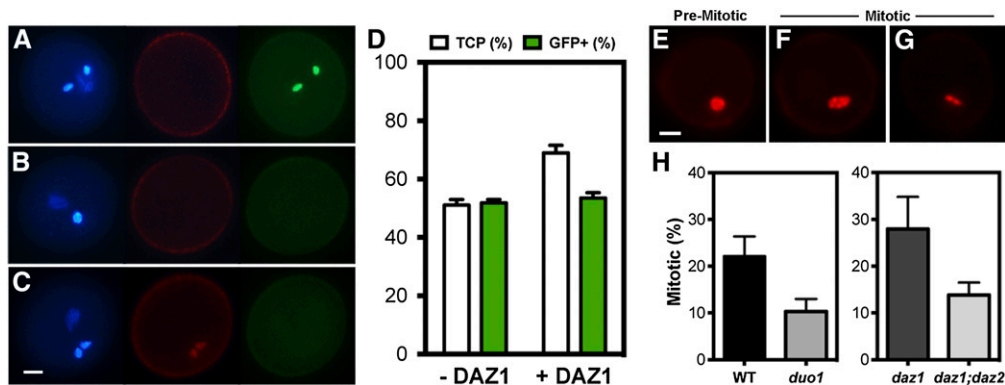
Construct	T1 Lines	Total (<i>n</i>)	% Tricellular	χ^2 Analysis	
				χ^2	Significance
DAZ1 full length	6	1201	69.4	181.590	***
mEAR-1	4	841	59.7	31.592	***
mEAR-2	4	869	63.5	63.550	***
mEAR-1,2	4	705	55.7	9.306	**
Δ EAR-1,2	4	672	53.0	2.381	ns

ProDAZ1:DAZ1-mCherry and variant transgenes were introduced into *daz1-1^{-/-} daz2-1^{+/-}* plants and pollen from single locus T1 lines scored for bicellular pollen by fluorescence microscopy; *n* = total pollen counted. χ^2 analysis was used to test for significant deviation from the expected ratio of 1:1 if there was no rescue of failed division (i.e., 50% tricellular and 50% bicellular pollen); ***P* < 0.01, ****P* < 0.001. ns, not significant.

double homozygous mutants were identified, and the segregation of genotypes deviated significantly from that expected in an F2 population (*n* = 187, $\chi^2 = 42.6$, *P* < 0.001) (Supplemental Table 3), indicating that the *daz1 daz2* double mutant allele combination is not transmitted through pollen. This was confirmed in a test cross of *ms1-1^{-/-} × daz1-1^{+/-} daz2-1^{-/-}*, since double heterozygotes were absent from F1 progeny (Supplemental Table 4).

The failure to transmit *daz1 daz2* double mutant alleles could result from the delivery of single mutant germ cells and/or the failure of fertilization arising from incomplete cell differentiation. When we dissected mature green siliques from homozygous-heterozygous mutants (e.g., *daz1-1^{+/-} daz2-1^{-/-}*), we observed a high proportion of aborted ovules that were not evident in siliques from wild-type and single *daz1-1^{-/-}* or *daz2-1^{-/-}* plants (Figures 6A and 6B). To establish whether *daz1 daz2* mutant pollen tubes are guided to ovules, we crossed *ms1-1^{-/-}* pistils with *daz1-1^{+/-} daz2-1^{-/-}* plants and stained pollen tubes 1 d after

pollination. We observed that pollen tubes were associated with 96.9% \pm 1.6% (\pm SD, *n* = 200) of developing seeds. The majority of ovules arising from crosses with wild-type or *daz2-1* pollen showed endosperm proliferation and the presence of a globular embryo (Figures 6C and 6D). In contrast, a significant proportion of ovules arising from crosses with *duo1-4^{+/-}* and *daz1-1^{+/-} daz2-1^{-/-}* plants showed unfertilized eggs and central cell nuclei (Figures 6E and 6F). The frequency of unfertilized ovules was 41.8 and 34.9%, respectively, which is less than the 50% expected based on the 1:1 segregation of wild-type and mutant pollen (Figure 6G). These data are consistent with the secondary fertilization of some ovules by wild-type pollen tubes after initial entry of a mutant pollen tube (Beale et al., 2012; Kasahara et al., 2012). To directly investigate fertilization, we used a semi-in vitro assay (Kasahara et al., 2012) to observe the fate of single *daz1 daz2* gametes released into the embryo sac. Briefly, sperm nuclei were labeled with ProDUO1:H2B-tdTomato and nuclei of female gametophyte accessory cells were labeled with ProACT11:H2B-GFP.

**Figure 4.** DAZ1/DAZ2 Promotes Germ Cell Division but Not Differentiation in the Absence of DUO1.

(A) Wild-type pollen is tricellular with ProHTR10:H2B-GFP expression.

(B) *duo1-1* pollen is bicellular with no ProHTR10:H2B-GFP activity.

(C) Expression of ProDUO1:DAZ1-mCherry in *duo1-1* rescues germ cell division, but the *HTR10* marker is not expressed. Bar = 5 μ m.

(D) Frequency of tricellular pollen and ProHTR10:H2B-GFP-expressing (GFP+) pollen in *duo1-1* plants, with (+DAZ) or without (-DAZ) the rescuing ProDUO1:DAZ1-mCherry transgene. Error bars represent the SE. *n* \geq 6 lines.

(E) to (G) Condensation of the germ cell nucleus, marked with ProDUO1:H2B-tdTomato, during G2- to M-phase transition. Germ cell chromatin in premitotic nuclei (E) is condensed during prophase (F) and further compacted as chromosomes congress at metaphase (G). Bar = 10 μ m.

(H) The percentage of mitotic germ cells in developing anthers of wild-type, *duo1-4^{+/-}*, *daz1-1^{-/-}*, and *daz1-1^{-/-} daz2-1^{+/-}* plants. Error bars represent the SE.

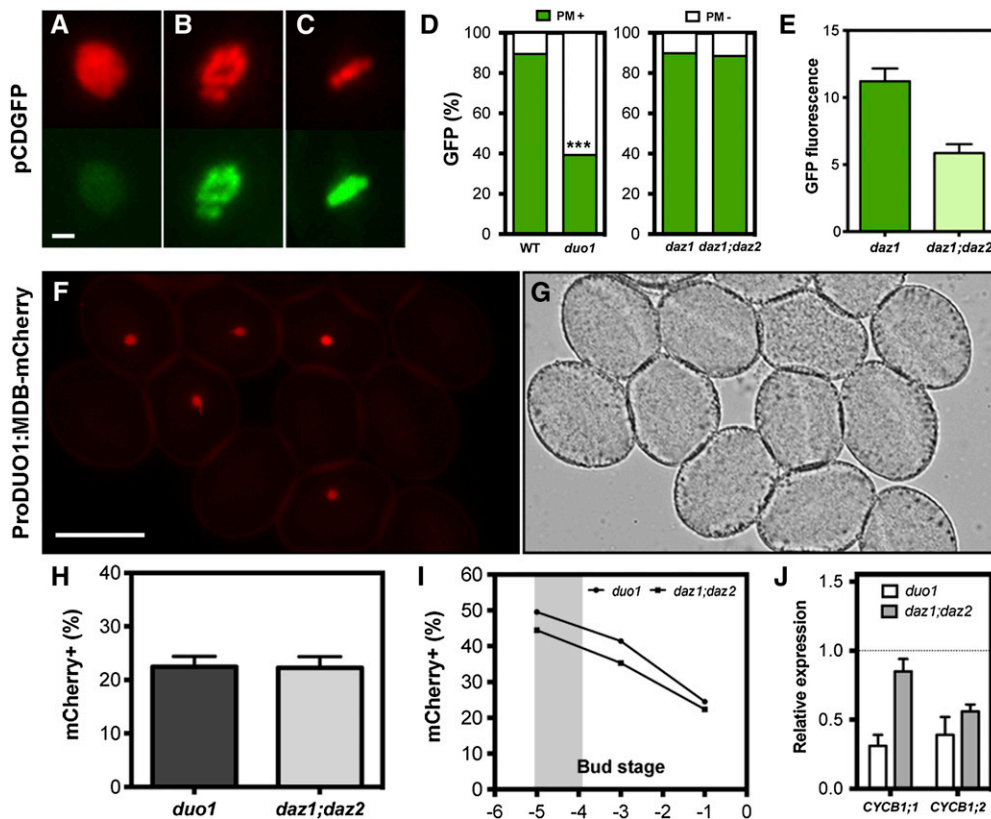


Figure 5. DAZ1 and DAZ2 Are Required for the Accumulation of Mitotic Cyclins.

(A) to (C) ProCYCB1;1:MDB-GFP expression during the G₂- to M-phase transition. GFP is first detected in nuclei of premitotic cells (A) and increases in cells undergoing mitosis (B) and (C). Corresponding nuclear phenotypes are marked with ProDUO1:H2B-tdTomato. Bar = 5 μ m.

(D) Frequency of premitotic (PM) cells with (PM+, green) and without (PM-, white) ProCYCB1;1:MDB-GFP expression. Anthers enriched with mitotic cells were analyzed from at least two independent lines of wild-type, *duo1-4^{+/-}*, *daz1-1^{-/-}*, and *daz1-1^{-/-} daz2-1^{+/-}*. Asterisks indicate a significant difference in the ratio observed in *duo1-4^{+/-}* anthers compared with the wild type ($\chi^2 = 149.77$, ***P < 0.001).

(E) Reduced accumulation of ProCYCB1;1:MDB-GFP in premitotic germ cells of *daz1-1^{-/-} daz2-1^{+/-}* anthers compared with *daz1-1^{-/-}* anthers. Error bars represent the SE. *n* > 25.

(F) and (G) Fluorescence (F) and DIC (G) image of mature pollen from *duo1-4^{+/-}* plants showing that ProDUO1:MDB-mCherry expression only persists in mutant germ cells. Bar = 30 μ m.

(H) Frequency of germ cells with persistent ProDUO1:MDB-mCherry signal (mCherry+) in mature pollen. Data represent means of T1 lines (*n* > 6) for *duo1-4^{+/-}* and *daz1-1^{+/-} daz2-1^{-/-}*. Error bars represent the SE.

(I) Frequency of germ cells with a ProDUO1:MDB-mCherry signal in successive bud stages. Anthers were dissected from staged buds of a representative T1 line for *duo1-4^{+/-}* and *daz1-1^{-/-} daz2-1^{+/-}*. Gray shading indicates the developmental window of germ cell mitosis.

(J) Reduced CYCB1;1 and CYCB1;2 transcript levels in pollen from *duo1-4^{+/-}* and *daz1-1^{+/-} daz2-1^{-/-}* plants. Data from qRT-PCR analysis are presented as fold change relative to the wild type, and error bars represent the SE of six biological replicates.

In six observations of single gamete discharge, fertilization of the egg or central cell did not occur (Figures 6H to 6M; Supplemental Movie 1 and 2), similar to previous observations of mutant *duo3* germ cells and *gcs1/hap2* sperm cells (Kasahara et al., 2012).

Given that *daz1 daz2* double mutant gametes are not competent for fertilization, we monitored gamete differentiation by introducing markers for two DUO1 target genes, the male gamete-specific histone H3.3 variant *HTR10/MGH3* (Okada et al., 2005) and the sperm plasma membrane protein *GCS1/HAP2*, which is required for gamete fusion (Mori et al., 2006; von Besser et al., 2006). All *daz1 daz2* germ cells expressed ProHTR10:H2B-GFP (Figure 7A),

although quantification of GFP fluorescence indicated a significant reduction in expression compared with sperm cells (Figure 7B). In contrast, the ProHAP2:HAP2-eYFP marker was only expressed in ~35% of *daz1 daz2* germ cells, and yellow fluorescent protein (YFP) was reduced by ~6.5-fold (Figure 7D). Transcript levels in pollen for these and three other DUO1 target genes (*TIP5;1*, *OPT8*, and *PCR11*) were reduced approximately 2-fold in *daz1-1^{+/-} daz2-1^{-/-}* and *duo1-4^{+/-}* plants. Transcript levels for *MYB101*, a gene with vegetative cell-specific expression in pollen, remained unchanged (Figure 7G) (Leydon et al., 2013).

We hypothesized that DUO1 expression might be suppressed in *daz1 daz2* germ cells because of the reduced expression of

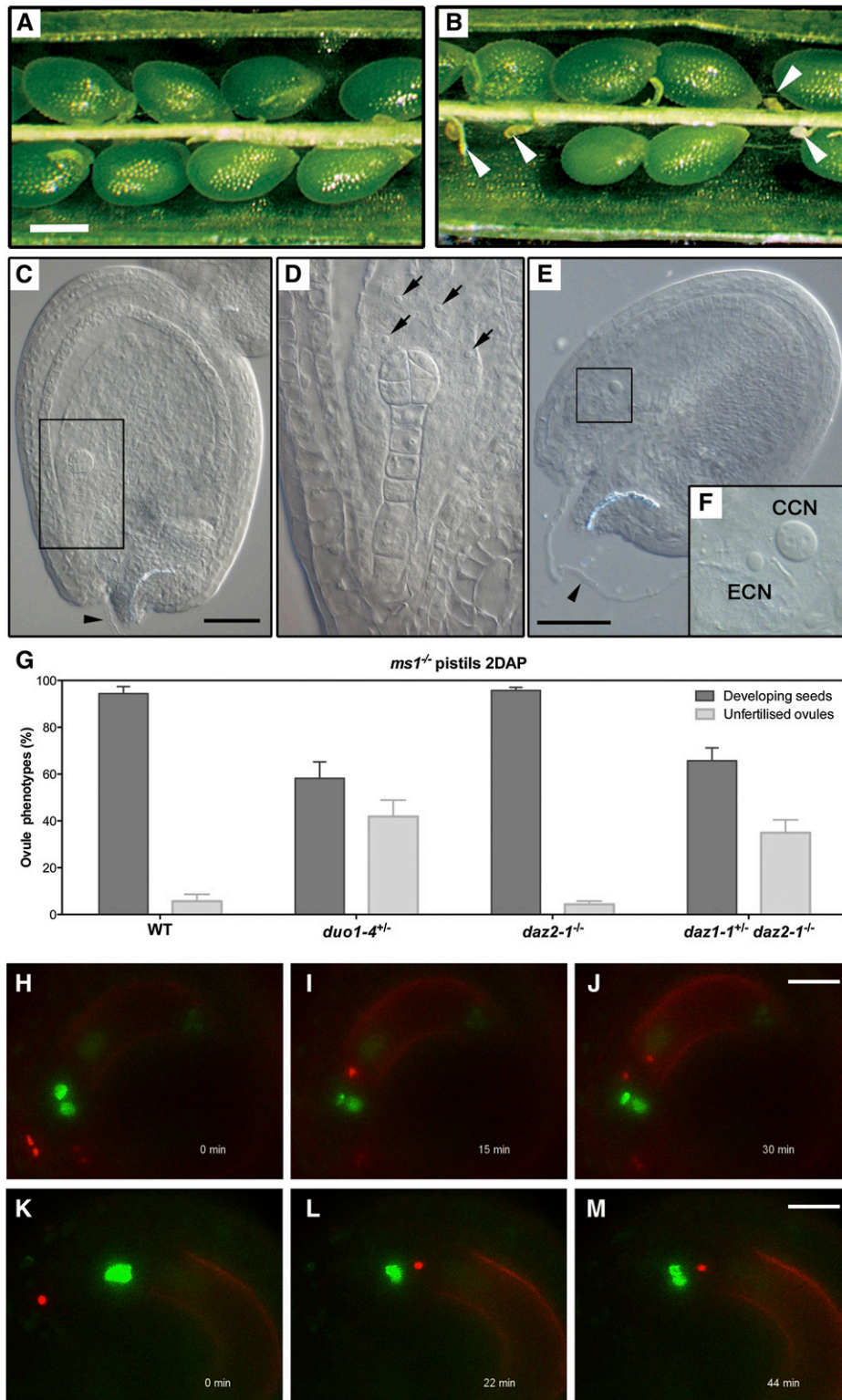


Figure 6. Mutant *daz1 daz2* Germ Cells Are Not Competent for Fertilization.

(A) and **(B)** Mature siliques from self fertilized *daz1-1^{+/-} daz2-1^{-/-}* mutant plants **(B)** contained aborted ovules (white arrowheads) as well as normal seeds similar to those of the wild type **(A)**. Bar = 200 μ m.

DUO1-dependent genes. When the expression of a ProDUO1:DUO1-mCherry marker was monitored, we observed DUO1 expression in all *daz1 daz2* germ cells (Figure 7E), but unexpectedly DUO1-mCherry fluorescence was significantly increased in *daz1 daz2* germ cells compared with sperm (Figure 7F). This was reflected by an increase in *DUO1* transcript levels in *daz1-1^{+/-} daz2-1^{-/-}* pollen compared with the wild type (Figure 7G). These data show that the differentiation of *daz1 daz2* germ cells is incomplete and suggest that DAZ1/DAZ2-dependent pathways limit the expression of DUO1.

DAZ1/DAZ2 Are Transcriptional Repressors That Interact with the Corepressor TOPLESS

We tested the potential interactions of DAZ1 and DAZ2 with the TPL/TPR family of corepressors in quantitative yeast two-hybrid assays. The N-terminal region of TPL contains a CTLH domain responsible for interaction with EAR motifs (Szemenyei et al., 2008). When this TPL fragment was used as prey with full-length DAZ1 or DAZ2 as bait, we observed increases of 5.5- and 17.6-fold in β -gal activity, respectively (Figures 8A and 8B). We tested the importance of the EAR motifs in DAZ1 by mutating the first (mEAR-1), the second (mEAR-2), or both (mEAR-1,2) to alanine-rich regions that are known to disrupt EAR function (Figure 8A) (Hiratsu et al., 2004). Mutation of one or both EAR motifs resulted in β -gal activity similar to that from strains without TPL prey, demonstrating their importance for the physical interaction of DAZ1 with TPL (Figure 8B).

To assess the ability of DAZ1 to act as a trans-acting transcriptional repressor, we used an *Arabidopsis* protoplast transfection assay (Ohta et al., 2001). A fusion of the DAZ1 C-terminal region with the GAL4 DNA binding domain repressed an ERF5-activated reporter gene (Figure 8C). This repression was dependent on the integrity of a single EAR domain as only mutagenesis of both (mEAR-1,2) could restore luciferase activity to steady state levels (Figure 8C). These results demonstrate that the DAZ1 and DAZ2 EAR domains can function as transcriptional repressors.

We tested the EAR dependence of DAZ1 and DAZ2 function using in planta complementation, in which the ability of mEAR variants to rescue failure of germ cell division in *daz1-1^{-/-} daz2-1^{+/-}* plants was scored (Figure 8A, Table 1). Full-length DAZ1-mCherry was able to completely rescue division of *daz1 daz2* germ cells, but plants expressing mEAR-1 or mEAR-2 showed a reduced efficiency of 50 and 69.7%, respectively

(Figure 8D, Table 1). Mutation of both EAR domains (mEAR-1,2) resulted in the least efficient rescue, with only 29.6% of mutant germ cells dividing to form two sperm cells (Figure 8D, Table 1). Finally, when we expressed a DAZ1 fusion protein lacking the C terminus (Δ EAR-1,2), we observed no deviation in the frequency of pollen with undivided germ cells compared with nonrescued plants (Figure 8D, Table 1). These results demonstrate that the integrity of both EAR motifs is essential for germ cell division.

To examine whether rescued *daz1 daz2* sperm cells were capable of fertilization, we monitored the transmission of DAZ1-mCherry variants through pollen. Hemizygous lines expressing DAZ1-mCherry variants were used as pollen donors and the progeny scored for antibiotic resistance. Full-length DAZ1 was able to fully rescue transmission, since a 2:1 ratio of resistant-to-sensitive seedlings was observed (Table 2). mEAR-1 and mEAR-2 lines showed reduced transmission efficiency of 63.0 and 37.5%, respectively (Figure 8D). Mutation or truncation of both EAR motifs had a more severe effect on transmission, with mEAR-1,2 and Δ EAR-1,2 showing 8.9 and 21.7%, respectively (Figure 8D). We conclude that the EAR motifs have an important role in DAZ1 function in germ cell division and sperm fertility.

DISCUSSION

DAZ1 and DAZ2 Are Male Germline-Specific Regulatory Proteins

We identified a subordinate regulatory node in the DUO1 network that constitutes a pair of redundant EAR motif-containing C₂H₂-type zinc finger proteins, DAZ1 and DAZ2. Our findings provide insights into their mechanisms of action and the regulatory hierarchy directing proliferation and differentiation of the male germ cell lineage. *DAZ1* and *DAZ2* transcripts were undetectable in the sporophyte, and protein fusions for both genes were specifically expressed in the male germline (Figure 1B). This parallels the expression of *DUO1* and is consistent with the evidence that DUO1 directly regulates the expression of *DAZ1* and *DAZ2*. First, the activity of the *DAZ1* and *DAZ2* promoters is suppressed in mutant *duo1* germ cells (Borg et al., 2011); second, DUO1-dependent activation of both promoters involves multiple MYB binding sites (Figure 2), which are also required for the germline-specific expression of the DUO1 target *HTR10/ MGH3* (Borg et al., 2011).

Figure 6. (continued).

(C) to (F) DIC images of cleared ovules 2 d after pollination with wild-type pollen showing proliferating endosperm (black arrows) and a dermatogen stage embryo ((C) and (D)). Pollination with *daz1-1^{+/-} daz2-1^{-/-}* plants resulted in a class of small ovules with an unfertilized egg and central cell nucleus ((E) and (F)). The black arrowhead indicates a penetrating pollen tube. ECN, egg cell nucleus; CCN, central cell nucleus. Bars = 100 μ m.
(G) Frequency of ovule phenotypes observed 2 d after pollination in crosses between *ms1^{-/-}* pistils and pollen from wild-type, *duo1-4^{+/-}*, *daz2-1^{-/-}*, and *daz1-1^{+/-} daz2-1^{-/-}* plants. Error bars represent the SE ($n = 5$ siliques).
(H) to (J) Time-lapse images showing the discharge of two *daz1* sperm cells, followed by syngamy and movement of sperm cell nuclei. Gamete nuclei (red) were labeled with ProDUO1:H2B-tdTomato. Nuclei of female gametophyte accessory cells (green) were labeled with ProACT11:H2B-GFP. Time elapsed shown is 0 min (H), 15 min (I), and 30 min (J). Bar = 20 μ m.
(K) and (L) Time-lapse images showing the discharge of single *daz1 daz2* germ cells and failure of fertilization. The movie was captured with the same experimental setup and originated from the same flower shown in images (H) to (J). Time elapsed shown is 0 min (K), 15 min (L), and 30 min (M). Bar = 20 μ m.

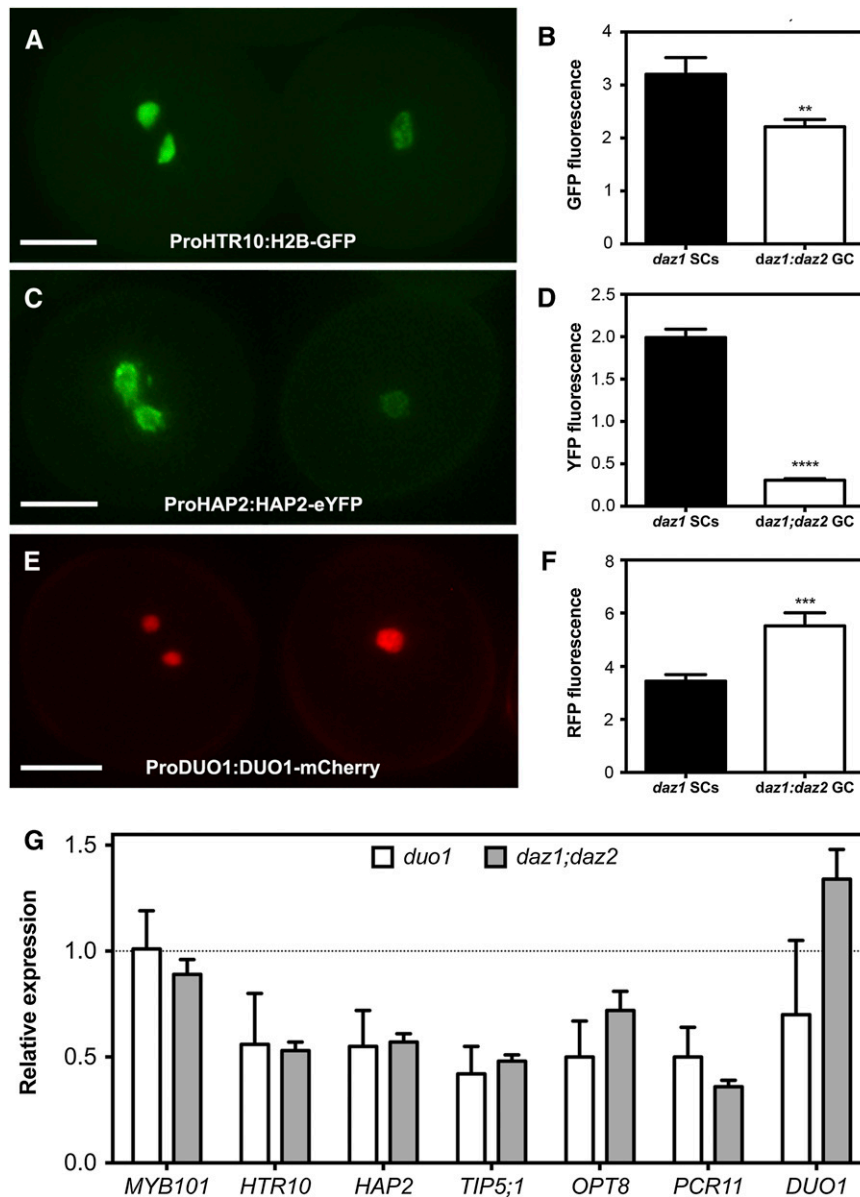


Figure 7. DAZ1/DAZ2-Dependent Pathways Influence Sperm Cell Differentiation.

(A) to (F) Images show the expression of gamete differentiation markers in *daz1-1* sperm cells (left) and *daz1-1 daz2-1* germ cells (right). The levels of fluorescence are shown in the corresponding bar chart. Relative to *daz1-1* sperm cells, marker expression was reduced in *daz1-1 daz2-1* germ cells for ProHTR10:H2B-GFP (A) and (B); Welch's *t* test, $**P < 0.01$) and ProHAP2:HAP2-eYFP (C) and (D); Welch's *t* test, $****P < 0.0001$), and increased for ProDUO1:DUO1-mCherry (E) and (F); Welch's *t* test, $***P < 0.001$). Error bars represent the \pm SE, $n > 30$. Bars = 10 μ m.

(G) Relative transcript levels of gamete differentiation genes in pollen from *duo1-4^{+/-}* and *daz1-1^{+/-} daz2-1* plants determined by qRT-PCR analysis. *HTR10*, *HAP2*, *TIP5;1*, *OPT8*, and *PCR11* are all germline-specific DUO1 target genes, and *MYB101* is a vegetative cell-specific gene. Values are shown as fold change difference relative to the wild type. Error bars represent the \pm SE of six biological replicates.

Several lines of evidence support the hypothesis that DAZ1 and DAZ2 act as transcriptional repressors. First, DAZ1 and DAZ2 fusion proteins are enriched in sperm cell nuclei and are similar to transcriptional repressors which combine C₂H₂-type zinc finger and EAR motifs (Bowman et al., 1992; Hiratsu et al., 2004; Payne et al., 2004; Weingartner et al., 2011). Second, we showed that the EAR motifs of DAZ1 are required to direct

transcriptional repression (Figure 8C) and that DAZ1 and DAZ2 can interact with the N-terminal region of the corepressor TOPLESS in an EAR-dependent manner (Figure 8B). Third, transcripts of the TPL/TPR gene family are expressed in sperm cells (Borges et al., 2008), making them strong candidates to support the EAR-dependent functions of DAZ1 and DAZ2. Importantly, we showed that the integrity of the EAR motifs in

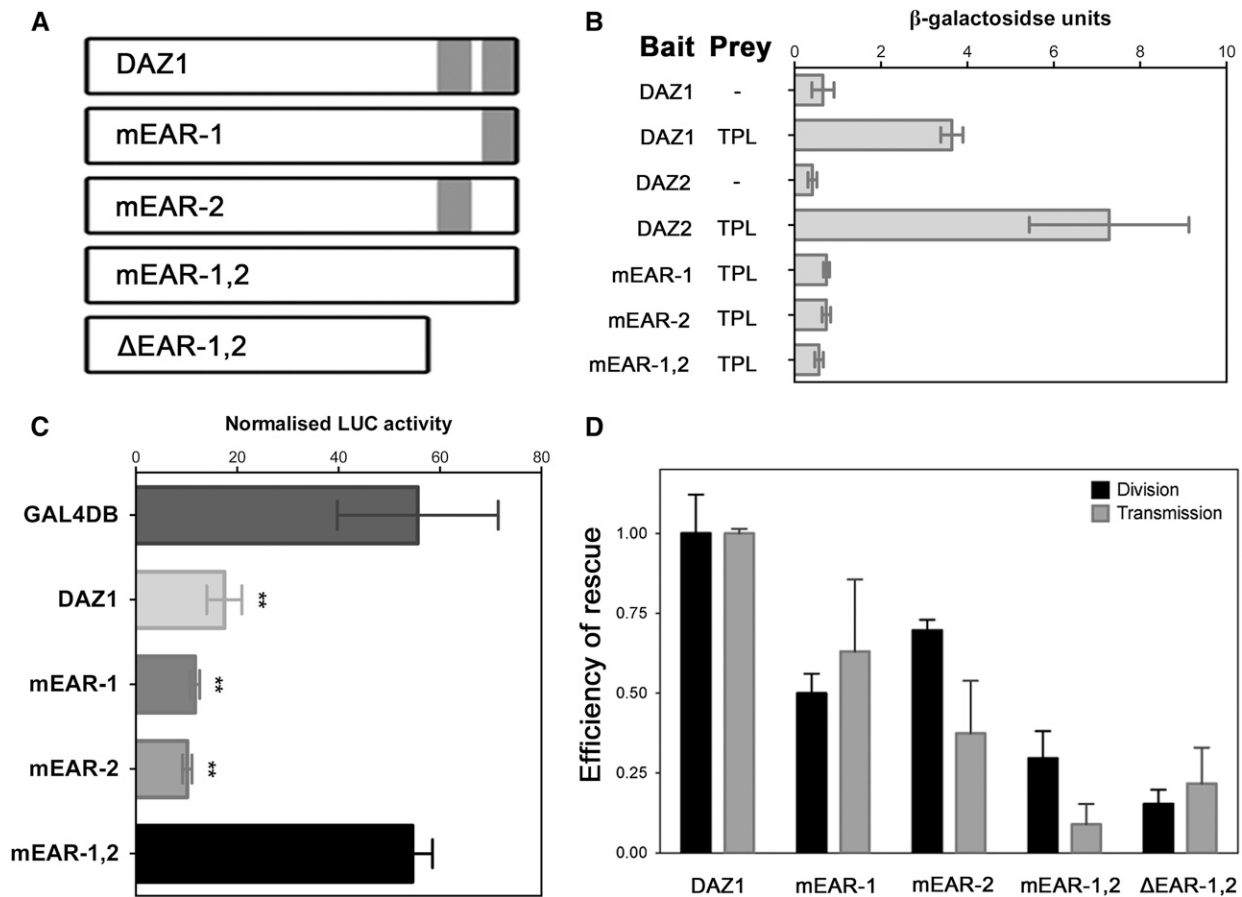


Figure 8. DAZ1 Function Involves EAR-Mediated Mechanisms That Are Important for Male Germline Development.

(A) Schematic diagram of the DAZ1 protein and DAZ1 variants in which the tandem EAR motifs (gray shading) are mutated independently (mEAR-1 and mEAR-2) and in combination (mEAR-1,2) or both deleted (ΔEAR-1,2).

(B) Yeast two-hybrid analysis of TPL interaction with DAZ1 and DAZ2. The N-terminal region of TPL (amino acids 1 to 226) was used as prey and DAZ1 variants as bait. Values represent the mean β -galactosidase activity of three technical replicates and error bars the sd .

(C) DAZ1 repression activity in *Arabidopsis* protoplasts. The luciferase reporter gene is driven by a chimeric promoter containing multiple GAL4 and ERF5-responsive binding sites (Ohta et al., 2001). Relative luciferase activity after cotransfection with 35S-ERF5 and each 35S-GAL4DB-DAZ1 variant is presented. Values represent the mean of four technical replicates and error bars the se .

(D) Functional analysis of the EAR motifs in DAZ1 by in planta complementation. The ProDAZ1:DAZ1-mCherry transgene and mEAR variants were introduced into *daz1-1^{-/-} daz2-1^{+/-}* plants. Rescue of germ cell division was determined from the percentage of tricellular pollen, whereas rescue of male transmission was determined from the inheritance of transgene-linked antibiotic resistance. Results are presented as rescue efficiency relative to full-length DAZ1 protein, and error bars represent the se . $n = 4$ T1 lines for analysis of division rescue and $n > 200$ seedlings for analyses of male transmission.

DAZ1 is required to promote mitotic division and gamete differentiation (Figure 8D), suggesting that the role of DAZ1 and DAZ2 in the germline most likely operates through mechanisms involving TPL/TPR-mediated transcriptional repression.

A DUO1-DAZ1/DAZ2 Regulatory Module Controls Germ Cell G2/M-Phase Transition

Whereas a robust molecular framework is emerging for the control of G1/S-phase transition in plants (Zhao et al., 2012), less is known about the regulatory modules promoting G2/M-phase transition (Berckmans and De Veylder, 2009). Our study provides insights into how cell type-specific mechanisms drive

G2/M-phase transition, and we propose that the DUO1-DAZ1/DAZ2 regulatory module controls mitotic division in the male germline (Figure 9). Several lines of evidence support the proposed model. First, the failure of *daz1 daz2* germ cells to enter mitosis is not due to incomplete replication, since mutant cells reenter S-phase after skipping mitosis (Figure 3K). Moreover, *daz1 daz2* germ cells show reduced mitotic B1-type cyclin expression, and endoreduplication is known to be associated with reduced G2/M-cyclin-dependent kinase activity (Cebolla et al., 1999; Kiang et al., 2009). Second, DAZ1/DAZ2-deficient germ cells fail to enter mitosis even though DUO1 is still expressed, and, importantly, the expression of DAZ1 in *duo1* mutant germ cells is able to restore mitotic division independently of gamete

Table 2. The EAR Motifs of DAZ1 Are Essential for Genetic Transmission

Construct	PPT ^R	PPT ^S	Ratio (R:S)	χ^2 Analysis	
				χ^2	Significance
DAZ1 full length	194	98	1.9:1	0.01	ns
mEAR-1	296	190	1.6:1	7.26	**
mEAR-2	434	339	1.3:1	38.51	***
mEAR-1,2	378	357	1.1:1	76.80	***
Δ EAR-1,2	248	213	1.2:1	34.36	***

Two single locus T1 lines expressing DAZ1-mCherry and mEAR-mCherry variant transgenes in the *daz1-1^{-/-} daz2-1^{+/-}* background were used as pollen donors in a cross to *ms1*. The number and ratio (R:S) of resistant (PPT^R) and sensitive (PPT^S) F1 seedlings is shown. χ^2 analysis was used to test for significant deviation from the expected ratio of 2:1 if transmission was fully rescued; **P < 0.01, ***P < 0.001. ns, not significant.

differentiation. Third, despite increased levels of DUO1 and low APC/C activity in *daz1 daz2* germ cells, expression of CYCB1;1 was unable to rescue mitotic division, unlike the incomplete rescue observed in *duo1* germ cells (Brownfield et al., 2009a). This was in contrast to our expectation that increased activity of the DUO1 promoter in *daz1 daz2* mutant cells might increase the efficiency of rescue compared with *duo1*, supporting the conclusion that reduced accumulation of CYCB1;1 is not the primary cause of failed division in *daz1 daz2*. It is notable that some DAZ1 and DAZ2 promoter activity remains in mutant *duo1* germ cells (Borg et al., 2011), suggesting that residual DAZ1/DAZ2 activity could support the partial rescue of germ cell division in *duo1* by CYCB1;1 and that DAZ1/DAZ2 are required to regulate other factors to promote germ cell mitosis. Thus, we propose that DAZ1/DAZ2-dependent repression of unknown inhibitory factors promotes the activity of G2/M-promoting factors including CYCB1;1 and CYCB1;2.

DAZ1 and DAZ2 Are Required for Sperm Cell Differentiation and Fertility

We showed that DAZ1/DAZ2-deficient germ cells are successfully discharged into embryo sacs but do not undergo syngamy. Consistent with this, *daz1 daz2* germ cells are incompletely differentiated as several DUO1 target genes are downregulated, but unexpectedly *DUO1* expression is increased (Figure 7). Thus, our findings implicate DAZ1/DAZ2-dependent repression in a feedback loop that attenuates *DUO1* expression and facilitates the expression of DUO1 target genes during sperm cell development (Figure 9). Consequently, the DAZ1/DAZ2 node is sufficient to promote G2/M-phase transition but is also required to ensure gamete specification. Consistent with this, DAZ1 can rescue division of *duo1* germ cells to form sperm cells, but these fail to differentiate completely (Figures 4A to 4D).

The developmentally phased expression of DUO1 and DAZ1/DAZ2 (Figures 1C and 1D) supports the operation of mechanisms that limit DUO1 accumulation in sperm cells and is consistent with the role of DAZ1/DAZ2 in a feedback loop. A possible mechanism could involve stimulation of *DUO1* turnover via miR159-mediated regulation since the *DUO1* transcript contains a functional miR159 binding site (Palatnik et al., 2007). Borges et al. (2011) found that miR159a was significantly enriched in sperm cells and miR159-guided cleavage products as well as noncanonical products were detected in wild-type

inflorescences and pollen (Grant-Downton et al., 2009; Allen et al., 2010). Furthermore, the *DUO1* promoter is sufficient to direct male germline-specific expression, suggesting that miR159-mediated regulation of *DUO1* may be restricted to the male germline (Brownfield et al., 2009a). Finally, increased expression of *DUO1* has been associated with reduced levels of APC/C and miR159 (Zheng et al., 2011). We thus speculate that DAZ1/DAZ2 might stimulate *DUO1* turnover via miR159-mediated regulation, consistent with the low levels of APC/C in mutant *duo1* and *daz1 daz2* germ cells (Figures 5F to 5J).

The failure of DAZ1/DAZ2-deficient cells to differentiate completely could operate through the repression of factors that limit expression of germline genes such as chromatin-remodeling

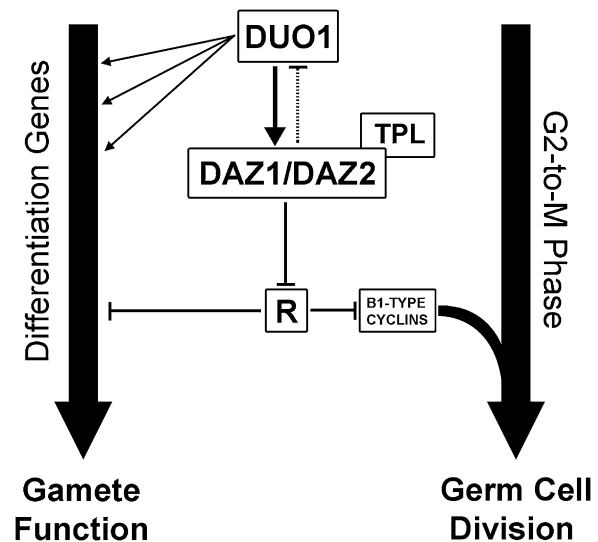


Figure 9. The DAZ1/DAZ2 Regulatory Node Is Essential for Sperm Cell Development.

Expression of DUO1 in generative (germ) cells activates genes required for gamete specification, including DAZ1 and DAZ2. DAZ1/DAZ2 occupy a distinct node in the DUO1 network to counteract repressive mechanisms (R) via EAR-dependent interaction with the corepressor TPL. DAZ1/DAZ2 overcomes a developmental block to sperm cell formation and maturation by (1) facilitating DUO1-dependent activation of gamete differentiation genes and the turnover of DUO1 and (2) the G2- to M-phase accumulation of mitotic cyclins to promote germ cell division.

factors. Transcriptional states are often dictated by the dynamic structure of chromatin and DAZ1/DAZ2 might stimulate epigenetic changes that promote interactions between DUO1 and its target promoters. Alternatively, it is possible that DAZ1/DAZ2 could function as a bifunctional activator-repressor similar to the role of EAR-containing WUSCHEL in stem cell regulation and floral patterning (Ikeda et al., 2009). Identification of the target genes directly regulated by DAZ1/DAZ2 is therefore key to building a robust network model of regulation in male germline development.

Our findings provide insights into the hierarchy and modulation of plant germline regulatory networks and implicate gene repression mechanisms in cellular proliferation and gamete specification. DUO1 acts as a network trigger in male germline development, which sets up and later responds to the DAZ1/DAZ2 node to ensure germ cell division and correct specification of the gametes. The deep phylogenetic conservation of DUO1 and DAZ1/DAZ2 in the angiosperms suggests that the DUO1-DAZ1/DAZ2 regulatory module is an ancient feature of plant male germline development.

METHODS

Plant Material and Growth Conditions

Arabidopsis thaliana plants were grown on soil in greenhouse conditions (21 to 25°C) with a 16-h photoperiod or in growth chambers at 24°C under continuous illumination (120 to 140 mmol/m²/s with 60% humidity). *duo1-1* has been described previously (Durbary et al., 2005), and *duo1-4* is a newly described ethyl methanesulfonate-induced Col-0 allele (a C-to-T mutation at position 545 creates a premature stop codon). The *daz1* and *daz2* alleles were obtained from the SALK T-DNA insertion collection (*daz1-1*, SALK_058012; *daz1-2*, SALK_151422; *daz2-1*, SALK_101906) (Scholl et al., 2000). Seeds of the ProHAP2:HAP2-eYFP marker line (von Besser et al., 2006) were kindly provided by Mark Johnson. Transgenic ProCYCB1;1:MDB-GFP, ProHTR10:H2B-GFP, and ProDUO1:CYCB1;1 lines have been described previously (Brownfield et al., 2009a, 2009b).

Genotyping and Selection of Transgenic Lines

Plants were genotyped for the *daz1-1*, *daz1-2*, and *daz2-1* allele using gene-specific primers in combination with the T-DNA border primer SALKLB1.3 (Supplemental Table 5). Plants harboring *daz1* and *daz2* alleles were transformed with vectors carrying the bar gene using the floral dip method (Clough and Bent, 1998) and T1 plants selected on soil subirrigated with 30 mg/mL Finale (glufosinate ammonium; DHA1 PROCIDA).

Molecular Cloning and Vector Construction

Unless specified, constructs were generated by MultiSite Gateway Technology (Invitrogen) as described (Borg et al., 2011). Entry clones were generated for promoter regions (pDONRP4P1R), cDNAs (pDONR221), and fluorescent tags (pDONRP2R-P3) using primers with suitable *attB* adapters (Supplemental Table 5). The *DAZ1* and *DAZ2* upstream promoter regions and cDNAs were amplified from Col-0 genomic DNA. Promoter fragments with mutated MBSs and DAZ1 mEAR variants were generated by overlap extension PCR (Higuchi et al., 1988). The tdTomato clone was generated by amplification from a template kindly provided by Roger Tsien. The MDB-mCherry cDNA consisted of a direct translational fusion of residues 1 to 117 of the CYCB1;1 cDNA to the N-terminal region of mCherry. Entry clones for the *DUO1* promoter, H2B, GFP, mCherry, and

luciferase cDNA have been described previously (Brownfield et al., 2009b; Borg et al., 2011).

Entry clones were used to generate expression clones by recombination into T-DNA destination vectors pB7m34GW, pB7m24GW,3, and pK7m24GW,3 (Karimi et al., 2002). For the yeast two-hybrid vectors, full-length *DAZ1*, *DAZ2*, and *DAZ1* mEAR variants were recombined into pB27 bait vector and the N-terminal region of TPL (amino acids 1 to 226) were recombined into pP6 prey vector (both vectors kindly provided by Hybrigenics Services). The vectors used for protoplast repression assays (Ohta et al., 2001) were kindly provided by Masaru Ohme-Takagi (AIST, Tsukuba, Japan). In-frame fusions to GAL4DB were generated using the C-terminal region (241 to 270 amino acids) of *DAZ1* and mEAR variant cDNA clones. Fragments were amplified and inserted into 35S-GAL4DB using unique *SmaI-SalI* restriction sites. The pRT2 Ω RenLUC control for the repression assay was generated by replacement of firefly luciferase in pRT2 Ω LUC with an *NcoI-BamHI* renilla luciferase fragment from pBS-35S-RenLUC.

Microscopy, Developmental Analysis, and Live-Cell Imaging of Fertilization

Mature pollen was stained with DAPI as described previously (Park et al., 1998). For developmental analysis, anthers were dissected from buds at different stages of development as defined (Durbary et al., 2005). Spores were released into 0.3 M mannitol by slicing open anthers with a hypodermic needle on a microscope slide. The stage of pollen development was determined using differential interference contrast (DIC) and/or fluorescence microscopy using methods and equipment described by Brownfield et al. (2009a). Transmission electron microscopy was performed as described by Park and Twell (2001). Clearing and observation of developing ovules by DIC microscopy was performed as described by Park et al. (2004). Pollen tubes were visualized by aniline blue staining (Mori et al., 2006) and live-cell imaging was performed using the methods and equipment detailed by Hamamura et al. (2011). Briefly, sperm nuclei were labeled with ProDUO1:H2B-tdTomato, and nuclei of female gametophyte accessory cells were labeled with ProACT11:H2B-GFP.

Marker Line Analysis

Observations of ProCYCB1;1:MDB-GFP and ProDUO1:MDB-mCherry lines were performed after mounting spores and mature pollen in 0.3 M mannitol. For developmental analysis of ProCYCB1;1:MDB-GFP marker lines, buds enriched with cells in mitosis were identified using a second ProDUO1:H2B-tdTomato transgene, which marks germ cell chromatin. The developmental window occurs at around bud stage -4 to -5 (Durbary et al., 2005), and images were captured randomly under standard conditions to characterize the population and to quantify levels of ProCYCB1;1:MDB-GFP (see Fluorescence and DNA Content Measurements below).

For analysis of ProDUO1:MDB-mCherry marker lines, T1 plants were screened to identify *duo1* and *daz1 daz2* mutants based on a persistent mCherry signal in mutant germ cells, and their genotype was confirmed by independent observations of pollen with DAPI staining. Detailed counts were made of at least seven T1 lines that appeared single locus (i.e., 25% mCherry-positive mutant germ cells). For analysis of differentiation markers shown in Figure 7, lines were made homozygous in a *daz1-1^{-/-} daz2-1^{+/-}* background and images of mature pollen captured under standard conditions to quantify fluorescence levels (see Fluorescence and DNA Content Measurements below).

Complementation Analysis

Analysis of functional complementation lines (Figures 4 and 8) was performed essentially as described by Borg et al. (2011), and at least three independent T1 lines with single locus insertions (i.e., ~50% red

fluorescent protein-positive pollen grains) were scored. The efficiency of rescue of failed division was calculated as a percentage of the *daz1 daz2* pollen grains that inherit the transgene (i.e., ~25% of the total population), since pollen from a *daz1-1^{-/-} daz2-1^{+/-}* plant equally segregates *daz1* and *daz1 daz2* pollen and half of each genotype inherits the transgene. Similarly, the efficiency of rescue of male transmission was calculated as a proportion of antibiotic-resistant seedlings in the F1 progeny that can inherit *daz1 daz2* and the transgene (i.e., 16% of the progeny). This arises because transmission can only be restored to the 25% of the pollen population that is *daz1 daz2* and which inherits the transgene, such that antibiotic-resistant seedlings increase from 50% (no rescue) to a maximum of 66% (complete rescue).

Fluorescence and DNA Content Measurements

The relative DNA contents of mutant germ cell nuclei was measured based on the fluorescence of DAPI-stained nuclei essentially using methods described previously (Durbary et al., 2005; Brownfield et al., 2009b). Images were captured under standard conditions and analyzed using equipment and software described by Borg et al. (2011). The mean fluorescence of *duo2* mutant germ cell nuclei, which are arrested at prometaphase (2.0C) was used to calculate relative C-values (Durbary et al., 2005). Measurements of in planta levels of protein and promoter activity presented in Figures 1, 5, and 7 were based on measurements of fluorescence in sperm and/or germ cell nuclei performed as described (Borg et al., 2011).

qRT-PCR Analysis

qRT-PCR assays were performed using SYBR Green JumpStart Taq ReadyMix (Sigma-Aldrich) using 0.5 μ M of each primer per reaction. Primers were tested to ensure high efficiency (95 to 105%) by analyzing a standard curve of serially diluted cDNA, and dissociation curves were monitored to check homogeneity of the amplified samples.

For the developmental analysis (Figure 1), data were obtained using a PTC-200 Peltier Thermal Cycler (MJ Research) modified with a Chromo4 Continuous Fluorescence Detector module (MJ Research). cDNA generated from RNA of spore fractions enriched at four stages of pollen development (Honys and Twell, 2004) was analyzed in triplicate in 20- μ L reactions. The expression level was determined using the relative standard curve method (Chiyu et al., 2005) and values calculated by normalization to *HTR5* (At4g40040) in the same sample.

For analysis of transcript abundance in mutant pollen (Figures 5 and 7), data were obtained using a LightCycler 480 system (Roche). Pollen from six independent populations of wild-type, *duo1-4^{+/-}*, *daz1-1^{-/-}*, and *daz1-1^{+/-} daz2-1^{-/-}* plants were analyzed. RNA isolated with a Spectrum Plant Total RNA kit (Sigma-Aldrich) was used to generate cDNA for each population with M-MLV reverse transcriptase (Promega). Ten-microliter reactions were performed in triplicate in a 384-well format, and Best-Keeper software (Pfaffl et al., 2004) was used to confirm the stability of the reference genes *HTR5* and *VCK* (At2g24370) across the pollen genotypes. A reference index derived from both reference genes was calculated to determine target transcript abundance. Expression levels were determined from the C_p values of the six biological replicates relative to the wild type using REST software (Pfaffl et al., 2002).

Luciferase Assays

Transient luciferase assays were performed by agroinfiltration of tobacco (*Nicotiana tabacum*) leaves as described (Borg et al., 2011). Transcriptional repression assays were performed in protoplasts prepared using the *Arabidopsis*-tape sandwich method (Wu et al., 2009). Protoplasts were transfected using the polyethylene glycol-calcium method (Yoo et al., 2007). GAL4GCC-LUC reporter, 35S-ERF5 effector, 35S-GAL4DB effector, and pRT2 Ω RenLUC control plasmid DNAs were transfected at

a 4:2:3:2 molar ratio at a total of 4.5 μ g DNA per transfection. Four independent transfections were performed using 2×10^4 protoplasts per transfection. After incubation in the dark at room temperature overnight, protoplasts were harvested and lysed in $1 \times$ Passive Lysis Buffer (Promega). Dual luciferase assays were performed using buffers described by Borg et al. (2011) and measured in duplicate with a FluoSTAR luminometer plate reader (BMG Labtech). Results were confirmed in two independent assays.

Yeast Two-Hybrid Interactions

A LexA-based yeast two-hybrid system was used in this study. Yeast strain L40 Δ GAL4 (TATA; from Hybrigenics) was cotransformed with bait and prey plasmid combinations (see Molecular Cloning and Vector Construction) using methods described previously (Gietz and Woods, 2006). Transformants harboring both bait and prey plasmids were selected on plates containing minimal medium lacking Leu and Trp. A quantitative measurement of β -galactosidase activity was performed with a chlorophenolred- β -D-galactopyranoside assay (Invitrogen ProQuest Two-Hybrid System). For controls, empty prey vector pP6 was used as prey.

Phylogenetic and Statistical Analysis

To identify homologs, *Arabidopsis* DAZ1 and DAZ2 protein sequences were used in a BLASTp search of UNIPROTKB. Multiple alignment of amino acid sequences was performed using the MUSCLE algorithm with default settings in MacVector (version 12.6.0). Statistical analyses were performed using the graphing and statistical software package GraphPad Prism 5.0. Descriptive statistics were first performed to assess data normality using a D'Agostino-Pearson omnibus test and the variance equality assessed with Bartlett's test of homogeneity of variances. Statistical assessment of genetic data was performed with a χ^2 test using Microsoft Excel. All tests were two-sided with statistically significant outcomes determined using α level of 0.05.

Accession Numbers

Sequence data from this article can be found in the GenBank/EMBL libraries under the following accession numbers: AT1G68610 (*PCR11*), AT1G19890 (*HTR10/MGH3*), AT2G17180 (*DAZ1*), AT3G47440 (*TIP5;1*), AT3G60460 (*DUO1*), AT4G11720 (*HAP2/GCS1*), AT4G35280 (*DAZ2*), AT4G37490 (*CYCB1;1*), AT5G06150 (*CYCB1;2*), and AT5G53520 (*OPT8*).

Supplemental Data

The following materials are available in the online version of this article.

Supplemental Figure 1. Alignment of Selected Angiosperm DAZ1 and DAZ2 Homologs.

Supplemental Figure 2. DAZ1 and DAZ2 Promoter Activity in Developing Pollen.

Supplemental Figure 3. DAZ1 and DAZ2 Protein Distribution in Sperm Cells.

Supplemental Figure 4. RT-PCR Expression Analysis of DAZ1 and DAZ2.

Supplemental Figure 5. Characterization of T-DNA Insertion Lines in DAZ1 and DAZ2.

Supplemental Table 1. Complementation of *duo1* Pollen with ProDUO1:DAZ1-mCherry.

Supplemental Table 2. Complementation of *daz1 daz2* Pollen with ProDUO1:CYCB1;1.

Supplemental Table 3. Segregation of F2 Genotypes from *daz1-1^{+/-} daz2-1^{+/-}* F1 Plants.

Supplemental Table 4. Genetic Transmission Analysis of *daz1 daz2* Pollen.

Supplemental Table 5. Primers Used in This Study.

Supplemental Movie 1. Live-Cell Imaging of Successful Fertilization by *daz1* Sperm Cells.

Supplemental Movie 2. Live-Cell Imaging Showing Failure of Fertilization by *daz1 daz2* Germ Cells.

ACKNOWLEDGMENTS

We thank June Saddington at the University of Leicester Botanic Gardens for support with plant cultivation, Natalie Allcock at the University of Leicester Electron Microscope Facility, Centre for Core Biotechnology Services, for performing electron microscopy, Anna Sidorova for help constructing the tdTomato entry clone, and Man-Kim Cheung (UWE, Bristol, UK) for the construction of pRT2 Ω LUC. We thank Johannes Hanson (Umea University, Sweden) for the gift of pBS-35S-RenLUC and Mark Johnson (Brown University) for kindly providing the HAP2-YFP marker line. This work was supported by Grant BB/I011269/1 from the Biotechnology and Biological Sciences Research Council in the UK. The funders had no role in study design, data collection and analysis, decision to publish, or preparation of the article.

AUTHOR CONTRIBUTIONS

M.B., N.R., K.R., and D.T. conceived and designed experiments. M.B. performed the main experimental work. N.R. performed functional complementation with mEAR variants. S. Kagale and K.R. performed yeast two-hybrid experiments. Y.H. and T.H. performed live-cell observations of fertilization. M.G. measured fluorescence levels of differentiation markers. S. Kumar assisted with generating ProDUO1:MDB-mCherry lines. M.A.E.-F. assisted with constructs and assays of promoter luciferase activity. U.S. assisted with segregation analysis. W.S. generated *duo1-4*. M.B., N.R., S.K., K.R., and D.T. analyzed the data. M.B. prepared figures. M.B. and D.T. wrote the article.

Received March 5, 2014; revised April 11, 2014; accepted May 2, 2014; published May 29, 2014.

REFERENCES

- Allen, R.S., Li, J., Alonso-Peral, M.M., White, R.G., Gubler, F., and Millar, A.A. (2010). MicroR159 regulation of most conserved targets in *Arabidopsis* has negligible phenotypic effects. *Silence* **1**: 18.
- Beale, K.M., Leydon, A.R., and Johnson, M.A. (2012). Gamete fusion is required to block multiple pollen tubes from entering an *Arabidopsis* ovule. *Curr. Biol.* **22**: 1090–1094.
- Berckmans, B., and De Veylder, L. (2009). Transcriptional control of the cell cycle. *Curr. Opin. Plant Biol.* **12**: 599–605.
- Berger, F., and Twell, D. (2011). Germline specification and function in plants. *Annu. Rev. Plant Biol.* **62**: 461–484.
- Borg, M., Brownfield, L., Khatab, H., Sidorova, A., Lingaya, M., and Twell, D. (2011). The R2R3 MYB transcription factor DUO1 activates a male germline-specific regulon essential for sperm cell differentiation in *Arabidopsis*. *Plant Cell* **23**: 534–549.
- Borg, M., Brownfield, L., and Twell, D. (2009). Male gametophyte development: a molecular perspective. *J. Exp. Bot.* **60**: 1465–1478.
- Borg, M., and Twell, D. (2010). Life after meiosis: patterning the angiosperm male gametophyte. *Biochem. Soc. Trans.* **38**: 577–582.
- Borges, F., Gomes, G., Gardner, R., Moreno, N., McCormick, S., Feijó, J.A., and Becker, J.D. (2008). Comparative transcriptomics of *Arabidopsis* sperm cells. *Plant Physiol.* **148**: 1168–1181.
- Borges, F., Pereira, P.A., Slotkin, R.K., Martienssen, R.A., and Becker, J.D. (2011). MicroRNA activity in the *Arabidopsis* male germline. *J. Exp. Bot.* **62**: 1611–1620.
- Bowman, J.L., Sakai, H., Jack, T., Weigel, D., Mayer, U., and Meyerowitz, E.M. (1992). SUPERMAN, a regulator of floral homeotic genes in *Arabidopsis*. *Development* **114**: 599–615.
- Brownfield, L., Hafidh, S., Borg, M., Sidorova, A., Mori, T., and Twell, D. (2009a). A plant germline-specific integrator of sperm specification and cell cycle progression. *PLoS Genet.* **5**: e1000430.
- Brownfield, L., Hafidh, S., Durberry, A., Khatab, H., Sidorova, A., Doerner, P., and Twell, D. (2009b). *Arabidopsis* DUO POLLEN3 is a key regulator of male germline development and embryogenesis. *Plant Cell* **21**: 1940–1956.
- Brownfield, L., and Twell, D. (2009). A dynamic DUO of regulatory proteins coordinates gamete specification and germ cell mitosis in the angiosperm male germline. *Plant Signal. Behav.* **4**: 1159–1162.
- Causier, B., Ashworth, M., Guo, W., and Davies, B. (2012). The TOPLESS interactome: a framework for gene repression in *Arabidopsis*. *Plant Physiol.* **158**: 423–438.
- Cebolla, A., Vinardell, J.M., Kiss, E., Oláh, B., Roudier, F., Kondorosi, A., and Kondorosi, E. (1999). The mitotic inhibitor *ccs52* is required for endoreduplication and ploidy-dependent cell enlargement in plants. *EMBO J.* **18**: 4476–4484.
- Chiyu, Z., Shungao, X., and Xinxiang, H. (2005). A novel and convenient relative quantitative method of fluorescence real time RT-PCR assay based on slope of standard curve. *Sheng Yu Hua Xue Yu Sheng Wu Wu Li Jin Zhan* **32**: 883–888.
- Clough, S.J., and Bent, A.F. (1998). Floral dip: a simplified method for *Agrobacterium*-mediated transformation of *Arabidopsis thaliana*. *Plant J.* **16**: 735–743.
- Dickinson, H.G., and Grant-Downton, R. (2009). Bridging the generation gap: flowering plant gametophytes and animal germlines reveal unexpected similarities. *Biol. Rev. Camb. Philos. Soc.* **84**: 589–615.
- Durberry, A., Vizir, I., and Twell, D. (2005). Male germ line development in *Arabidopsis*. *duo* pollen mutants reveal gametophytic regulators of generative cell cycle progression. *Plant Physiol.* **137**: 297–307.
- Engbrecht, C.C., Schoof, H., and Böhm, S. (2004). Conservation, diversification and expansion of C2H2 zinc finger proteins in the *Arabidopsis thaliana* genome. *BMC Genomics* **5**: 39.
- Gietz, R.D., and Woods, R.A. (2006). Yeast transformation by the LiAc/SS Carrier DNA/PEG method. *Methods Mol. Biol.* **313**: 107–120.
- Grant-Downton, R., Hafidh, S., Twell, D., and Dickinson, H.G. (2009). Small RNA pathways are present and functional in the angiosperm male gametophyte. *Mol. Plant* **2**: 500–512.
- Gross-ardt, R., Kägi, C., Baumann, N., Moore, J.M., Baskar, R., Gagliano, W.B., Jürgens, G., and Grossniklaus, U. (2007). LACHESIS restricts gametic cell fate in the female gametophyte of *Arabidopsis*. *PLoS Biol.* **5**: e47.
- Gusti, A., Bamberger, N., Nowack, M., Pusch, S., Eisler, H., Potuschak, T., De Veylder, L., Schnittger, A., and Genschik, P. (2009). The *Arabidopsis thaliana* F-box protein FBL17 is essential for progression through the second mitosis during pollen development. *PLoS ONE* **4**: e4780.
- Hamamura, Y., Saito, C., Awai, C., Kurihara, D., Miyawaki, A., Nakagawa, T., Kanaoka, M.M., Sasaki, N., Nakano, A., Berger, F., and Higashiyama, T. (2011). Live-cell imaging reveals the dynamics of two sperm cells during double fertilization in *Arabidopsis thaliana*. *Curr. Biol.* **21**: 497–502.

- Higuchi, R., Krummel, B., and Saiki, R.K.** (1988). A general method of in vitro preparation and specific mutagenesis of DNA fragments: study of protein and DNA interactions. *Nucleic Acids Res.* **16**: 7351–7367.
- Hiratsu, K., Mitsuda, N., Matsui, K., and Ohme-Takagi, M.** (2004). Identification of the minimal repression domain of SUPERMAN shows that the DLELRL hexapeptide is both necessary and sufficient for repression of transcription in Arabidopsis. *Biochem. Biophys. Res. Commun.* **321**: 172–178.
- Hony, D., and Twell, D.** (2004). Transcriptome analysis of haploid male gametophyte development in Arabidopsis. *Genome Biol.* **5**: R85.
- Ikeda, M., Mitsuda, N., and Ohme-Takagi, M.** (2009). Arabidopsis WUSCHEL is a bifunctional transcription factor that acts as a repressor in stem cell regulation and as an activator in floral patterning. *Plant Cell* **21**: 3493–3505.
- Kagale, S., Links, M.G., and Rozwadowski, K.** (2010). Genome-wide analysis of ethylene-responsive element binding factor-associated amphiphilic repression motif-containing transcriptional regulators in Arabidopsis. *Plant Physiol.* **152**: 1109–1134.
- Kagale, S., and Rozwadowski, K.** (2011). EAR motif-mediated transcriptional repression in plants: an underlying mechanism for epigenetic regulation of gene expression. *Epigenetics* **6**: 141–146.
- Karimi, M., Inzé, D., and Depicker, A.** (2002). GATEWAY vectors for Agrobacterium-mediated plant transformation. *Trends Plant Sci.* **7**: 193–195.
- Kawahara, R.D., Maruyama, D., Hamamura, Y., Sakakibara, T., Twell, D., and Higashiyama, T.** (2012). Fertilization recovery after defective sperm cell release in Arabidopsis. *Curr. Biol.* **22**: 1084–1089.
- Kiang, L., Heichinger, C., Watt, S., Bähler, J., and Nurse, P.** (2009). Cyclin-dependent kinase inhibits reinitiation of a normal S-phase program during G2 in fission yeast. *Mol. Cell. Biol.* **29**: 4025–4032.
- Kim, H.J., Oh, S.A., Brownfield, L., Hong, S.H., Ryu, H., Hwang, I., Twell, D., and Nam, H.G.** (2008). Control of plant germline proliferation by SCF(FBL17) degradation of cell cycle inhibitors. *Nature* **455**: 1134–1137.
- Leydon, A.R., Beale, K.M., Woroniecka, K., Castner, E., Chen, J., Horgan, C., Palanivelu, R., and Johnson, M.A.** (2013). Three MYB transcription factors control pollen tube differentiation required for sperm release. *Curr. Biol.* **23**: 1209–1214.
- Lieber, D., Lora, J., Schrempf, S., Lenhard, M., and Laux, T.** (2011). Arabidopsis WIH1 and WIH2 genes act in the transition from somatic to reproductive cell fate. *Curr. Biol.* **21**: 1009–1017.
- Lituiev, D.S., Krohn, N.G., Müller, B., Jackson, D., Hellriegel, B., Dresselhaus, T., and Grossniklaus, U.** (2013). Theoretical and experimental evidence indicates that there is no detectable auxin gradient in the angiosperm female gametophyte. *Development* **140**: 4544–4553.
- Mori, T., Kuroiwa, H., Higashiyama, T., and Kuroiwa, T.** (2006). GENERATIVE CELL SPECIFIC 1 is essential for angiosperm fertilization. *Nat. Cell Biol.* **8**: 64–71.
- Ohta, M., Matsui, K., Hiratsu, K., Shinshi, H., and Ohme-Takagi, M.** (2001). Repression domains of class II ERF transcriptional repressors share an essential motif for active repression. *Plant Cell* **13**: 1959–1968.
- Okada, T., Endo, M., Singh, M.B., and Bhalla, P.L.** (2005). Analysis of the histone H3 gene family in Arabidopsis and identification of the male-gamete-specific variant AtMGH3. *Plant J.* **44**: 557–568.
- Pagnussat, G.C., Alandete-Saez, M., Bowman, J.L., and Sundaresan, V.** (2009). Auxin-dependent patterning and gamete specification in the Arabidopsis female gametophyte. *Science* **324**: 1684–1689.
- Palatnik, J.F., Wollmann, H., Schommer, C., Schwab, R., Boisbouvier, J., Rodriguez, R., Warthmann, N., Allen, E., Dezulian, T., Huson, D., Carrington, J.C., and Weigel, D.** (2007). Sequence and expression differences underlie functional specialization of Arabidopsis microRNAs miR159 and miR319. *Dev. Cell* **13**: 115–125.
- Park, S.K., Howden, R., and Twell, D.** (1998). The *Arabidopsis thaliana* gametophytic mutation gemini pollen1 disrupts microspore polarity, division asymmetry and pollen cell fate. *Development* **125**: 3789–3799.
- Park, S.K., Rahman, D., Oh, S.A., and Twell, D.** (2004). gemini pollen 2, a male and female gametophytic cytokinesis defective mutation. *Sex. Plant Reprod.* **17**: 63–70.
- Park, S.K., and Twell, D.** (2001). Novel patterns of ectopic cell plate growth and lipid body distribution in the Arabidopsis gemini pollen1 mutant. *Plant Physiol.* **126**: 899–909.
- Pauwels, L., et al.** (2010). NINJA connects the co-repressor TOPLESS to jasmonate signalling. *Nature* **464**: 788–791.
- Payne, T., Johnson, S.D., and Koltunow, A.M.** (2004). KNUCKLES (KNU) encodes a C2H2 zinc-finger protein that regulates development of basal pattern elements of the Arabidopsis gynoecium. *Development* **131**: 3737–3749.
- Pfaffl, M.W., Horgan, G.W., and Dempfle, L.** (2002). Relative expression software tool (REST) for group-wise comparison and statistical analysis of relative expression results in real-time PCR. *Nucleic Acids Res.* **30**: e36.
- Pfaffl, M.W., Tichopad, A., Prgomet, C., and Neuvians, T.P.** (2004). Determination of stable housekeeping genes, differentially regulated target genes and sample integrity: BestKeeper—Excel-based tool using pair-wise correlations. *Biotechnol. Lett.* **26**: 509–515.
- Rabiger, D.S., and Drews, G.N.** (2013). MYB64 and MYB119 are required for cellularization and differentiation during female gametogenesis in *Arabidopsis thaliana*. *PLoS Genet.* **9**: e1003783.
- Rotman, N., Durbarry, A., Wardle, A., Yang, W.C., Chaboud, A., Faure, J.E., Berger, F., and Twell, D.** (2005). A novel class of MYB factors controls sperm-cell formation in plants. *Curr. Biol.* **15**: 244–248.
- Scholl, R.L., May, S.T., and Ware, D.H.** (2000). Seed and molecular resources for Arabidopsis. *Plant Physiol.* **124**: 1477–1480.
- Szemeyei, H., Hannon, M., and Long, J.A.** (2008). TOPLESS mediates auxin-dependent transcriptional repression during Arabidopsis embryogenesis. *Science* **319**: 1384–1386.
- Twell, D.** (2011). Male gametogenesis and germline specification in flowering plants. *Sex. Plant Reprod.* **24**: 149–160.
- von Besser, K., Frank, A.C., Johnson, M.A., and Preuss, D.** (2006). Arabidopsis HAP2 (GCS1) is a sperm-specific gene required for pollen tube guidance and fertilization. *Development* **133**: 4761–4769.
- Weingartner, M., Subert, C., and Sauer, N.** (2011). LATE, a C(2)H(2) zinc-finger protein that acts as floral repressor. *Plant J.* **68**: 681–692.
- Wu, F.-H., Shen, S.-C., Lee, L.-Y., Lee, S.-H., Chan, M.-T., and Lin, C.-S.** (2009). Tape-Arabidopsis Sandwich - a simpler Arabidopsis protoplast isolation method. *Plant Methods* **5**: 16.
- Yadegari, R., and Drews, G.N.** (2004). Female gametophyte development. *Plant Cell* **16** (suppl.): S133–S141.
- Yoo, S.-D., Cho, Y.-H., and Sheen, J.** (2007). Arabidopsis mesophyll protoplasts: a versatile cell system for transient gene expression analysis. *Nat. Protoc.* **2**: 1565–1572.
- Zhao, X., Harashima, H., Dissmeyer, N., Pusch, S., Weimer, A.K., Bramsiepe, J., Bouyer, D., Rademacher, S., Nowack, M.K., Novak, B., Sprunck, S., and Schnittger, A.** (2012). A general G1/S-phase cell-cycle control module in the flowering plant *Arabidopsis thaliana*. *PLoS Genet.* **8**: e1002847.
- Zheng, B., Chen, X., and McCormick, S.** (2011). The anaphase-promoting complex is a dual integrator that regulates both MicroRNA-mediated transcriptional regulation of cyclin B1 and degradation of Cyclin B1 during Arabidopsis male gametophyte development. *Plant Cell* **23**: 1033–1046.